Available online at www.sciencedirect.com
SciVerse ScienceDirect
Ceramics International 38 (2012) 3707–3711
CERAMICS INTERNATIONAL
www.elsevier.com/locate/ceramint

Electrophoretic deposition of $CoFe_2O_4$ films from aqueous suspensions

Gang Jian, Jun Zhao, Dongxiang Zhou, Qiuyun Fu *

Department of Electronic Science and Technology, Huazhong University of Science and Technology, 1037 Luoyu Road, Wuhan, Hubei 430074, PR China

Received 23 September 2011; received in revised form 12 December 2011; accepted 5 January 2012
Available online 14 January 2012

Abstract

$CoFe_2O_4$ nano-particles with average size of ~40 nm were synthesized via the chemical coprecipitation method. PAMA–NH_4 was used as dispersant to improve the stability of aqueous suspensions. Zeta potential and sediment volumes were tested to study the effects of pH and dispersant amounts on the stability of suspensions. The most stable suspension was obtained when using 0.6 wt.% PAMA–NH_4 as dispersant at pH = 10. Conductivity results showed that thoroughly dispersed suspensions were formed after being ultrasonic agitated for 30 min. $CoFe_2O_4$ films on Al_2O_3/Pt substrates fabricated via EPD sintered at 1250 °C exhibited preferentially oriented structure. The XRD analyses showed (2 2 0) and (5 1 1) were the preferential orientations. Anisotropy was also observed in magnetic hysteresis loops. Stronger ferromagnetic effect was observed in the in-plane orientation, with saturation magnetization of ~290 emu/cm^3.
© 2012 Elsevier Ltd and Techna Group S.r.l. All rights reserved.

Keywords: A. Suspensions; Electrophoretic deposition; $CoFe_2O_4$; Preferential orientations

1. Introduction

Co-ferrite has been a research focus for decades, because of its attractive properties, such as high Curie temperature, relatively high saturation magnetization, super-magnetostrictive property, and good chemical stability [1,2]. Co-ferrite films have practical applications in the magnetic recording, magnetic sensors, and multiferroic devices [1–4]. Electrophoretic deposition (EPD) is applicable to the production of $CoFe_2O_4$ films, which is realized via motions of charged particles in suspension towards an electrode under an applied electric field. The thrust of using the EPD technique to prepare thick films on conductive substrates is based on several attractive aspects such as high deposition rates, low apparatus cost, easy controllability of film thickness, and precise controllability of chemical composition [5,6]. However one problem with the EPD of magnetic particles is that stable suspensions with magnetic particles are harder to be prepared than those with only nonmagnetic particles as magnetic interactions exist besides van der Walls attractions. At present, most studies on the EPD of $CoFe_2O_4$ films have been conducted in organic solvents [7–9]. Although EPD of ceramic films such as $BaTiO_3$, Al_2O_3, and ZnO from aqueous has been reported [10–12], there is little literature of $CoFe_2O_4$ films aqueous deposited by EPD. EPD from aqueous suspensions has the advantage of low cost, high efficiency, and environmental benignity [10]. In this paper, $CoFe_2O_4$ films were fabricated via EPD in aqueous suspension. Anionic dispersant PAMA–NH_4 was added to improve the stability of suspension, and zeta potential combined with sediment volumes were studied in detail. Deposition kinetic behaviors were investigated. The microstructure of films was characterized by field-emission scanning electron microscopy (FESEM) and X-ray diffraction (XRD). The magnetic properties of films have also been analyzed.

2. Experimental

$CoFe_2O_4$ nano-particles were synthesized by the chemical coprecipitation method as the following process. At first, according to the Co/Fe ratio of 1:2, 0.267 mol/L $CoCl_2$ (0.1 mol) and 0.533 mol/L $FeCl_3$ (0.2 mol) aqueous solutions were prepared. 6 mol/L NaOH aqueous solution (0.44 mol) was also prepared as an oxidizer and pH adjuster. The NaOH solution was heated to 80 °C in a water bath, and then solutions of $CoCl_2$ and $FeCl_3$ were added slowly into the NaOH solution at the same time with stirring. Precipitation generated immediately. Then the mixture has been heated for more

* Corresponding author. Tel.: +86 27 87557447; fax: +86 27 87545167.
E-mail address: fuqy@mail.hust.edu.cn (Q. Fu).

0272-8842/$36.00 © 2012 Elsevier Ltd and Techna Group S.r.l. All rights reserved.
doi:10.1016/j.ceramint.2012.01.014

30 min. After that, the precipitation was washed and dried. The dried precipitation was calcinated at 800 °C for 2 h to form $CoFe_2O_4$ nano-particles.

The polished ITO conductive substrate and the Al_2O_3/Pt plate (1.5 cm × 2.5 cm) were used as the cathode and anode, respectively. The Al_2O_3 ceramics (99.5% purity) with density of 3.88 g/cm^3 was made by solid phase sintering method, and the surface of the ceramic was accurately polished. The Pt layer with thickness of ~1 μm was deposited on the Al_2O_3 ceramics by magnetron sputtering. The distance between two electrodes was fixed at 1.5 cm. A DC voltage power supplier (0–30 V) and a rectangular insulating tank were utilized for electrophoresis. Deionized water as solvent and PAMA–NH_4 as an anionic dispersant was used to prepare suspensions of $CoFe_2O_4$. Sediment volumes combined with zeta potential of suspensions were studied to analyze the stability of suspensions. Suspensions had to undergo physical dispersion such as ultrasonic agitation before deposition. In order to form thoroughly dispersed suspensions, ultrasonic agitation's effect on conductivity of suspensions was investigated.

The sediment volumes of suspensions were measured in 10 mL cylinders after being settled for 3 weeks. The suspension samples' concentration was 20 g/L. The particle size and zeta potential of suspensions was examined by a light scattering commercial device (Zetasizer 3000 HAS, Malvern Instruments Ltd., UK), and the suspension concentration was diluted to 10 mg/L before the particle size and zeta potential test. $NH_3{\cdot}H_2O$ was used to adjust the pH value. Viscosity of suspensions was measured by a rotary viscometer (NDJ-7, CN), a shear rate of 350 s^{-1} was chosen to compare the viscosities of different suspensions. The conductivity was measured by using a conductivity meter (DDB11-A, CN). Phase analysis was performed by XRD (X'Pert PRO) with Cu Ka X-ray. Microstructure images of the particles and films were observed by FESEM (Sirion 200 PRO). Magnetic hysteresis loop at room temperature was measured with a vibrating sample magnetometer (VSM) (Model 4HF).

3. Results and discussion

Fig. 1 exhibits the morphology and sizes of $CoFe_2O_4$ particles synthesized by the coprecipitation method. The SEM image showed that particles were regular and with spherical shape. The sizes of the particles examined by laser particle size analyzer showed that the mean particle size of $CoFe_2O_4$ powders was ~40 nm, which was in accordance with the result of SEM.

Stability of suspension was the key factor during EPD process. Suspensions with high stability are necessary to fabricate films with dense structure and ordered accumulation. In suspension of $CoFe_2O_4$, magnetic interactions besides van der Walls attraction existed which hampered the formation of stable suspension. In order to form stable suspension, anionic dispersant PAMA–NH_4 was used to provide larger inter-particle repulsive forces. PAMA–NH_4 was effective as a dispersant only in alkaline environment. Therefore, the pH value of suspensions was adjusted via addition of $NH_3{\cdot}H_2O$.

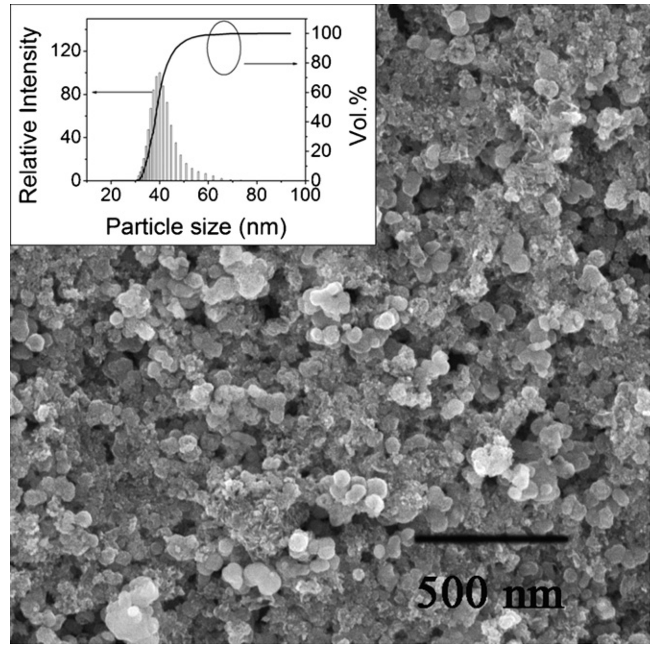

Fig. 1. Morphology of $CoFe_2O_4$ powders by SEM. In the inset the result measured by laser particle size analyzer.

The amount of PAMA–NH_4 and pH was tested for each experimental cycle, which is shown in Fig. 2. Sediment volume was taken to characterize the stability of suspensions. Generally, the more stable the suspension, the smaller the sediment volume [7,13].

Fig. 2 shows that the sediment volumes of $CoFe_2O_4$ suspensions decreased at low dispersant amounts and reached a minimum when dispersant amount was 0.6 wt.%. As dispersant amounts exceeded 0.6 wt.%, sediment volumes increase again. This could be explained by the hypothesis that the saturation adsorption amount of PAMA–NH_4 was 0.6 wt.%. For a fixed dispersant amount, the minimum sediment volume was found at pH of 10. It was concluded that $CoFe_2O_4$ suspension with 0.6 wt.% PAMA–NH_4 added at pH = 10 was with the highest stability.

Fig. 3 shows the viscosity and conductivity of $CoFe_2O_4$ suspensions with increasing PAMA–NH_4 amounts. The viscosity measurement was used to examine the adsorption

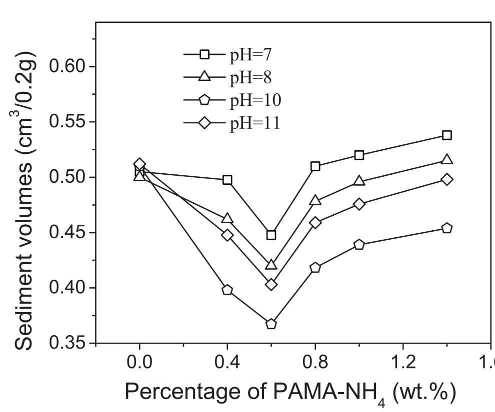

Fig. 2. Sediment volumes of $CoFe_2O_4$ suspensions with different PAMA–NH_4 amounts and pH.

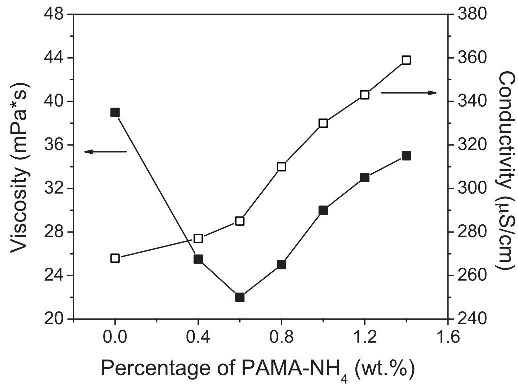

Fig. 3. Viscosity and conductivity of $CoFe_2O_4$ suspensions as a function of PAMA–NH_4 amounts.

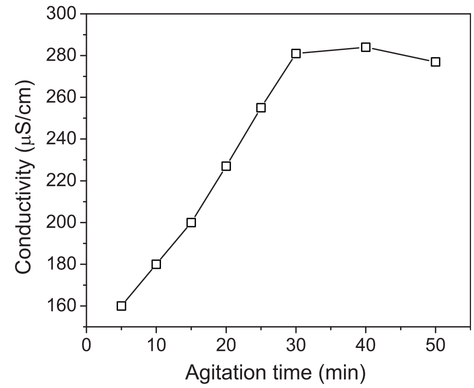

Fig. 5. Effect of ultrasonic agitation time on conductivity of suspensions.

of PAMA–NH_4 onto $CoFe_2O_4$ particles. The viscosity decreased and reached a minimum at PAMA–NH_4 amount of 0.6 wt.%, then it increased with increasing dispersant amounts. Thus we concluded that the saturation adsorption amount of PAMA–NH_4 onto $CoFe_2O_4$ particles was 0.6 wt.%. Conductivity of suspensions was relatively small before saturation adsorption of PAMA–NH_4 (0.6 wt.%), however it increased rapidly as dispersant addition exceeded 0.6 wt.%.

To prove the effect of pH on the stability of suspensions, zeta potential was also studied, as shown in Fig. 4. The zeta potential results were in accordance with results of sediment volumes in Fig. 2. The most stable suspension was formed at pH of 10, with zeta potential of −58 mV. The negative zeta potential values indicated particles were negatively charged in suspensions.

To get a thoroughly dispersed suspension, effect of ultrasonic agitation on the suspension's conductivity was studied, as shown in Fig. 5. With increased agitation time, the conductivity increased at first and then got saturated above 30 min. The trends of suspensions' conductivity were corresponding to the suspensions' dispersion degree. Thus the results showed that thoroughly dispersed suspensions had formed after 30 min agitation.

Fig. 6 depicts the kinetics of the $CoFe_2O_4$ deposition from aqueous suspensions. It showed that the deposition weight was in a nearly linear relationship with deposition time. The deposition weight increased as voltage changed from 2 to 4 V, while it decreased as voltage continued rising to 6 V. This attributed to the reason that the electrolysis of water occurred at high voltages, resulting in a less stable suspension and formation of porous films. Thus in our study, voltages in the range of 2–4 V were adopted. Fig. 6 indicates that film thickness may be controlled by changing of deposition time and voltage. It was possible to fabricate $CoFe_2O_4$ films with thickness from 0.5 to 30 μm by EPD.

Fig. 7 shows the microstructures of fabricated $CoFe_2O_4$ films on Al_2O_3/Pt substrates observed by SEM. Fig. 7(a) and (b) exhibits the surface images of as-deposited films. The deposited films showed homogeneous and dense structure. Fig. 7(c) and (d) exhibits surface images of $CoFe_2O_4$ films sintered at 1250 °C. It was observed that $CoFe_2O_4$ grains with size of 2–5 μm were orderly arranged in the films.

The phase analysis studied by XRD was shown in Fig. 8. All patterns were corresponding to cobalt ferrite spinel diffraction peaks. However, preferential orientations of sintered films were observed and compared with diffraction patterns of particles and as-deposited films. Table 1 shows the peaks' intensity of different samples extracted from results of Fig. 8. It showed that the peaks' intensities of (2 2 0) and (5 1 1) of sintered films were much higher than those of particles and as-deposited films. In other words, the sintered films showed preferentially oriented structure in (2 2 0) and (5 1 1).

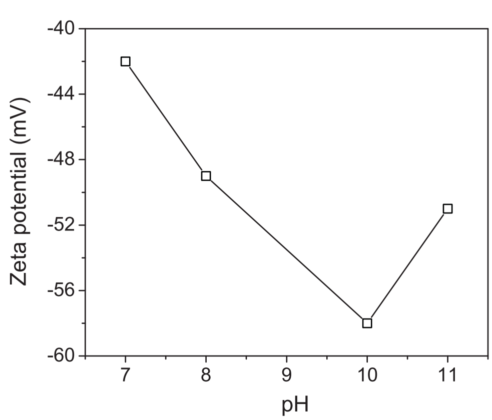

Fig. 4. Zeta potential of $CoFe_2O_4$ suspensions at different pH (PAMA–NH_4: 0.6 wt.%).

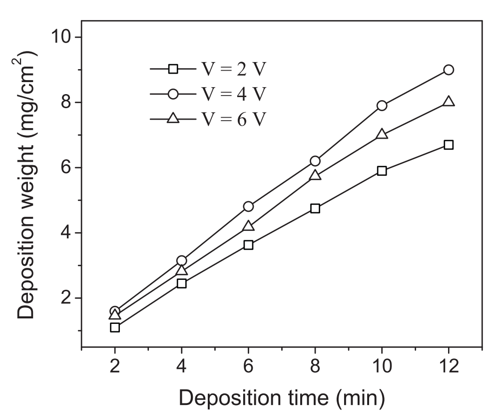

Fig. 6. Deposition weight as a function of deposition time at various voltages.

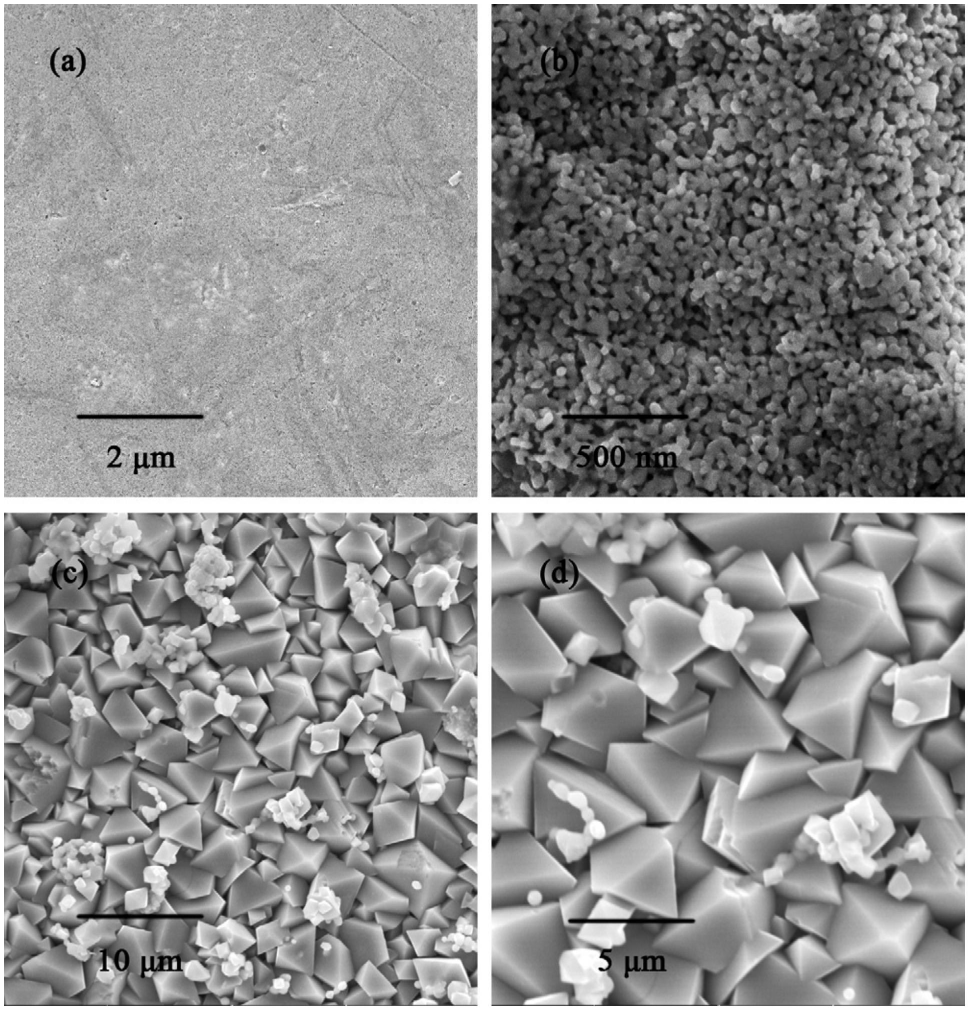

Fig. 7. SEM images of $CoFe_2O_4$ films: (a) and (b) as-deposited films, (c) and (d) films sintered at 1250 °C.

The oriented arrangement of $CoFe_2O_4$ grains could cause anisotropy of magnetic properties. To prove that, magnetic hysteresis loops of as-deposited films and sintered films were measured, as shown in Figs. 9 and 10. For both samples, magnetic hysteresis loops were measured in two different directions: in-plane and out-of-plane. The result in Fig. 9 indicates that the as-deposited films showed little anisotropy and with saturation magnetization of $\sim$220 emu/cm^3. Fig. 10 shows that evident anisotropy existed in sintered films. This could be attributed to two reasons: one lies in that the anisotropy was caused by substrate's clamping effect, as the sintered films showed stronger tightness with substrate than as-deposited films; the other is that the oriented growth of $CoFe_2O_4$ grains led to magnetic anisotropy. $CoFe_2O_4$ films with anisotropy caused by clamping effect showed only magnetic hysteresis loops' shape changes in different directions, but not drastic changes of saturation magnetization values [2,3,14]. As in Fig. 10 the sintered films' magnetic hysteresis loops in two directions not only exhibited shape changes but also had large difference in saturation magnetization values, so we concluded that the magnetic anisotropy in the sintered films was partly attributed to the ordered arrangement of $CoFe_2O_4$ grains. In Fig. 10, the saturation magnetization of sintered films were

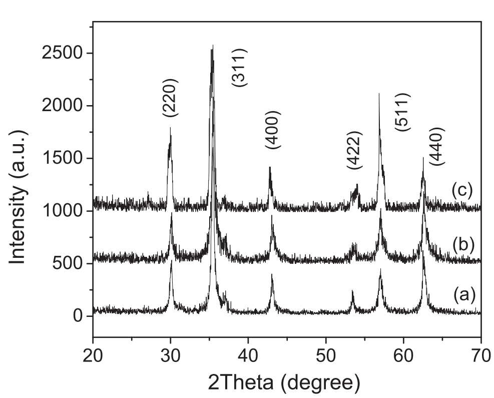

Fig. 8. XRD patterns of (a) $CoFe_2O_4$ particles, (b) as-deposited films, and (c) films sintered at 1250 °C.

Table 1
Intensity of diffraction peaks extracted from samples' XRD patterns.

	(2 2 0)	(3 1 1)	(4 0 0)	(4 2 2)	(5 1 1)	(4 4 0)
Particles	453	1568	398	219	419	616
As-deposited	447	1545	412	220	436	623
1250 °C	754	1539	381	214	718	610

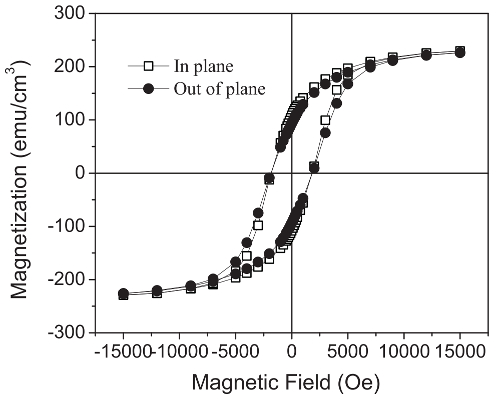

Fig. 9. Magnetic hysteresis loops (at room temperature) of as-deposited $CoFe_2O_4$ films.

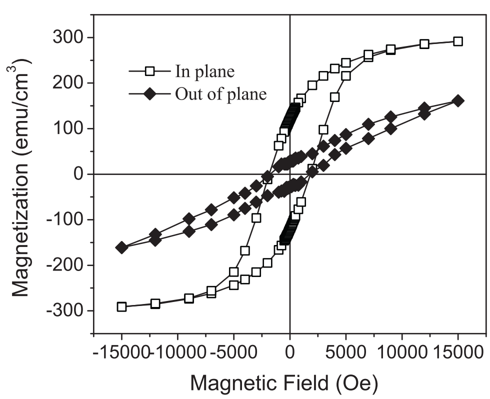

Fig. 10. Magnetic hysteresis loops (at room temperature) of sintered $CoFe_2O_4$ films (1250 °C).

$\sim$150 emu/cm^3 (out-of-plane) and $\sim$290 emu/cm^3 (in-plane), stronger ferromagnetic effect was observed in in-plane orientation.

4. Conclusions

Anionic dispersant PAMA–NH_4 was added to improve the stability of aqueous suspensions. Zeta potential and sediment volumes were tested to study the effect of pH and dispersant amounts on the stability of $CoFe_2O_4$ suspensions. The most stable suspension in this experiment was formed by using 0.6 wt.% PAMA–NH_4 as a dispersant at pH = 10. Conductivity results showed that thoroughly dispersed suspensions of $CoFe_2O_4$ were formed under ultrasonic agitation for at least 30 min. EPD was used to fabricate $CoFe_2O_4$ films, the kinetics shows that film thickness may be controlled by voltage and deposition time. $CoFe_2O_4$ films on Al_2O_3/Pt substrates sintered at 1250 °C exhibited preferentially oriented structure. The XRD analyses showed that (2 2 0) and (5 1 1) were the preferential orientations. Anisotropy was also observed in magnetic hysteresis loops, stronger ferromagnetic effect was observed in in-plane orientation, with saturation magnetization of $\sim$290 emu/cm^3.

Acknowledgments

This work was supported by the National Natural Science Foundation of China (Grant no. 60871017/f010612) and Provincial Nature Science Foundation of Hubei in China (Grant no. 2009CDB372).

References

[1] L.X. Phua, F. Xu, Y.G. Ma, C.K. Ong, Structure and magnetic characterizations of cobalt ferrite films prepared by spray pyrolysis, Thin Solid Films 517 (2009) 5858–5861.
[2] Y.C. Wang, J. Ding, J.B. Yi, B.H. Liu, T. Yu, Z.X. Shen, High-coercivity Co-ferrite thin films on (1 0 0)–SiO_2 substrate, Applied Physics Letters 84 (2004) 2596–2598.
[3] J.G. Lee, K.P. Chae, J.C. Sur, Surface morphology and magnetic properties of $CoFe_2O_4$ thin films grown by a RF magnetron sputtering method, Journal of Magnetism and Magnetic Materials 267 (2003) 161–167.
[4] A. Lisfi, C.M. Williams, Magnetic anisotropy and domain structure in epitaxial $CoFe_2O_4$ thin films, Journal of Applied Physics 93 (2003) 8143–8145.
[5] A. Wu, P.M. Vilarinho, S. Srinivasan, A.I. Kingon, I.M. Reaney, D. Woodward, A.R. Ramos, E. Alves, Microstructural studies of PZT thick films on Cu foils, Acta Materialia 54 (2006) 3211–3220.
[6] A. Wu, P.M. Vilarinho, Electrophoretic deposition of lead zirconate titanate films on metal foils for embedded components, Journal of the American Ceramic Society 89 (2006) 575–581.
[7] D.X. Zhou, G. Jian, Y.X. Hu, Y.N. Zheng, S.P. Gong, H. Liu, Electrophoretic deposition of multiferroic $BaTiO_3/CoFe_2O_4$ bilayer films, Materials Chemistry and Physics 127 (2011) 316–321.
[8] D.X. Zhou, G. Jian, Y.N. Zheng, S.P. Gong, F. Shi, Electrophoretic deposition of $BaTiO_3/CoFe_2O_4$ multiferroic composite films, Applied Surface Science 257 (2011) 7621–7626.
[9] W.F. Mo, J.W. Zhai, L. Zhang, X. Yao, Electric and magnetic properties of $CoFe_2O_4$–$PbZr_{0.5}Ti_{0.5}O_3$ composite thin films, Ferroelectrics 407 (2010) 54–60.
[10] J.L. Zhao, X.H. Wang, L.T. Li, Electrophoretic deposition of $BaTiO_3$ films from aqueous suspensions, Materials Chemistry Physics 99 (2006) 350–353.
[11] B. Ferrari, J.C. Farinas, R. Moreno, Determination and control of metallic impurities in alumina deposits obtained by aqueous electrophoretic deposition, Journal of the American Ceramic Society 84 (2001) 733–739.
[12] F. Tang, Y. Sakka, T. Uchikoshi, Electrophoretic deposition of aqueous nano-sized zinc oxide suspensions on a zinc electrode, Materials Research Bulletin 38 (2003) 207–212.
[13] M.C. Bennett, Zeta potential and sedimentation behaviour in flocculated Cane sugar juice, Nature 182 (1958) 1439–1440.
[14] X. Gao, B.J. Rodriguez, L. Liu, B. Birajdar, D. Pantel, M. Ziese, M. Alexe, D. Hesse, Microstructure and properties of well-ordered multiferroic Pb(Zr,Ti)$O_3/CoFe_2O_4$ nanocomposites, ACS Nano 4 (2010) 1099–1107.